

A Low Cost, Triple-Voltage Bus DC/DC Converter for Automotive Applications

Gui-Jia Su

National Transportation Research Center
Oak Ridge National Laboratory
2360 Cherahala Blvd., Knoxville, TN 37932
sugj@ornl.gov

Fang Z. Peng

Michigan State University
2120 Engineering Building
East Lansing, MI 48824-1226
fzpeng@egr.msu.edu

Abstract— Before the automotive industry completes moving the 14V vehicle loads to the 42V net, HEVs and fuel cell vehicles will likely employ a triple voltage - 14V/42V/High-voltage (200~500V) bus system. This paper presents a low-cost, soft-switched, bi-directional dc/dc converter for connecting the three voltage nets. The converter consists of two half-bridges and a high-frequency transformer, which provides voltage level matching and galvanic isolation between the two half-bridges for safety requirements. The use of dual half-bridges minimizes the number of switching devices and their associated gate drive components. Moreover, snubber capacitors and the transformer leakage inductance are utilized to achieve soft-switching. Therefore, no extra active switches or passive resonant components are required for soft-switching, further reducing component count. Control of power flow among the three voltage buses is achieved by adjusting the duty ratio and phase angle between the half-bridge output voltages. Simulation and experimental data on a 2 kW lab unit are included to verify the power flow control scheme.

Keywords-14V/42V/high-voltage dc/dc converter; EV/HEV dc/dc converter; power flow control; soft-switching

I. INTRODUCTION

Because the 14V electrical system in present automobiles has reached its limits of capability and cannot meet the demands of future electrical loads and the desire for replacing more engine driven mechanical and hydraulic systems with electrical systems to increase efficiency, the 42V power net has been proposed to cope with the increasing electrical loads. During the transition to the 42V system, most automobiles are expected to employ a 14V/42V dual-level voltage system, in which a bi-directional dc/dc converter is required to connect the two voltage networks [1][2]. Additionally, most battery powered hybrid electric vehicles (HEVs) employ a high voltage (200~500V) (H.V.) bus for the traction motor drive. In HEVs with a 42V alternator, a dc/dc converter supplied from the 42V bus may be used to charge the H.V. battery as

shown in Fig. 1(a). On the other hand, for HEVs having a generator directly connected on the H.V. bus, a dc/dc converter is typically required to charge the 14V and/or 42V batteries.

Furthermore, fuel cell powered vehicles will require a bi-directional dc/dc converter to interconnect the fuel cell powered H.V. bus and the low-voltage buses for vehicle auxiliary loads as shown in Fig. 1(b) [3-5]. An energy storage device is also required for fuel cell start-up and for storing the energy captured by regenerative braking because the fuel cells lack energy storage capability. One way to accomplish this is to utilize the vehicle 14V or 42V battery with the bi-directional dc/dc converter. During vehicle starting, the H.V. bus is boosted up to around 300V by the dc/dc converter drawing power from the 14V and/or 42V battery. This H.V. bus then supplies power for the fuel cell compressor motor expanding unit controller and brings up the fuel cell voltage, which in turn feeds back to the H.V. bus to release the loading from the battery [4][5].

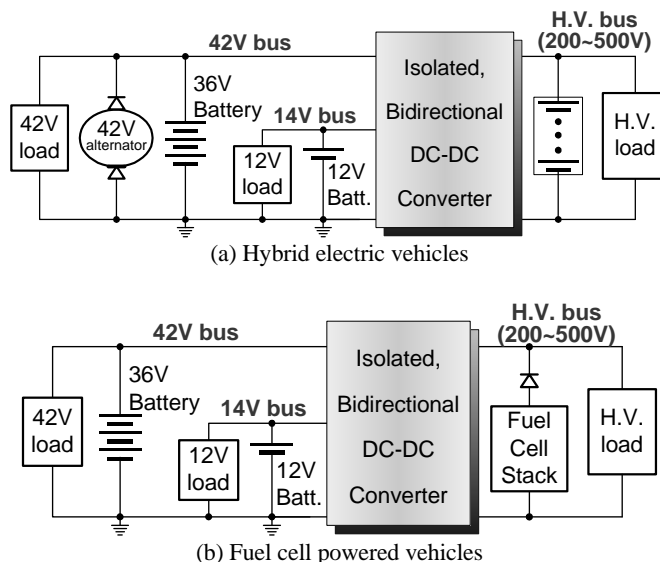


Fig. 1. A dc/dc converter interconnecting 14V/42V/ H.V. bus nets in HEVs and fuel cell powered vehicles.

* Prepared by Oak Ridge National Laboratory, managed by UT-Battelle, LLC, for the U.S. Dept. of Energy under contract DE-AC05-00OR22725. The submitted manuscript has been authored by a contractor of the U.S. Government under contract DE-AC05-00OR22725. Accordingly, the U.S. Government retains a nonexclusive, royalty-free license to publish or reproduce the published form of this contribution, or allow others to do so, for U.S. Government purposes.

In summary, a triple-voltage bus (14V/42V/H.V.) system will likely be employed in HEVs and fuel cell powered vehicles as shown in Fig. 1, before all vehicle auxiliary electrical components are moved to the 42V bus. While dc/dc converters are available to interconnect any two of the buses, to reduce component count, size, cost, and volume it is desirable to employ an integrated dc/dc converter to interconnect the three voltage buses instead of using two separate ones. Aside from bi-directional power flow control capability, the converter needs to provide galvanic isolation between the low-voltage and H.V. buses to meet safety requirements. Further, soft-switching is preferred over hard-switching because of the reduced level of electromagnetic interference (EMI) and switching losses with soft-switching [4-8].

This paper presents a low-cost, soft-switched, isolated bi-directional dc/dc converter for interconnecting the three bus nets. The converter is a modified version of the dual half-bridge topology proposed in [5]. It utilizes snubber capacitors and the transformer leakage inductance to achieve zero-voltage and/or zero-current switching. Therefore, no extra active switches or passive resonant components are required, further reducing component count. The inherent soft-switching capability and the low component count of the proposed converter allow high power density, efficient power conversion, and compact packaging. A novel power flow control scheme based on a combined duty ratio and phase shift angle control is also presented. A 2 kW lab unit is built and tested. Simulation and experimental data are included to verify the proposed power flow control scheme.

II. PROPOSED INTEGRATED DC/DC CONVERTER

A. Description of the Proposed DC/DC Converter

Fig. 2 shows a schematic of the dc/dc converter, which mainly consists of two half-bridge converters and a high-frequency transformer, T_r , that links the two half-bridges. The use of dual half-bridges minimizes the number of switching devices and their associated gate drive components. The high-frequency transformer provides the required galvanic isolation for safety requirements and voltage level matching between the 14V and 42V buses and the H.V. bus, while the 14V and 42V buses share a common ground. The leakage inductance of the transformer is utilized as the intermediate energy storing and transferring element between the two low-voltage buses and the H.V. net.

The half-bridge converter on the left side, consisting of two switches, S_1 and S_2 , and a voltage divider of two capacitors, C_1 and C_2 , connects directly to the 42V dc bus and through an inductor, L_{dc} , to the 14V dc bus. The left side converter thus not only generates an ac voltage of square wave, v_{TrL} to the transformer's primary winding, but also functions as a bi-directional chopper between the 14V and 42V buses. Control of the power flow between the low-voltage and H.V. sides can be achieved by adjusting the switches' duty cycle, the switching frequency, and/or the phase shift angle between the transformer primary and secondary voltages, as will be discussed in detail in the following sections.

The right side converter, also comprised of two switches, S_3 and S_4 , and two capacitors, C_3 and C_4 , connects directly to the 42V dc bus and through an inductor, L_{dc} , to the 14V dc bus. The left side converter thus not only generates an ac voltage of square wave, v_{TrL} to the transformer's primary winding, but also functions as a bi-directional chopper between the 14V and 42V buses. Control of the power flow between the low-voltage and H.V. sides can be achieved by adjusting the switches' duty cycle, the switching frequency, and/or the phase shift angle between the transformer primary and secondary voltages, as will be discussed in detail in the following sections.

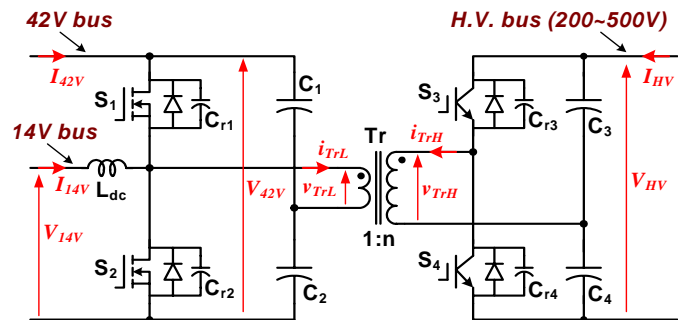


Fig. 2. Schematic of the soft-switched, bi-directional dc/dc converter for a triple-voltage bus system.

Across each switch there is a snubber capacitor including the parasitic capacitance of the device. The transformer leakage inductance, together with the snubber capacitors, $C_{r1} \sim C_{r4}$, is also utilized to provide soft-switching for the switches, eliminating the problems of interaction between the leakage inductance and diode reverse recovery. The resonance between the capacitors and the inductor enables the switches to turn on under zero current and voltage, while the snubber capacitors allow them to turn off at zero voltage. That is, turning off the conducting switch diverts the current to the associated snubber capacitors and charges it, resulting in a zero voltage turn-off. The diverted current simultaneously discharges the other capacitor of the same phase leg. Once the capacitor is fully discharged, the inductor current flows through the anti-parallel diode. The switch thus can be gated on under zero-voltage and zero-current while its diode is conducting. A step-by-step description of the soft-switching processes and soft-switching conditions are given in [5].

It is thus apparent that no additional active switches are needed for soft-switching. Moreover, no extra passive resonant components may be required because the transformer leakage inductance is used and the device's parasitic capacitance can be utilized as the snubber capacitors, further reducing component count. The inherent soft-switching capability and the low component count of the converter allows high power density, highly efficient power conversion, and compact packaging.

B. Equivalent Circuit and Power Flow Control

Because the phase leg of S_1 and S_2 acts as a bi-directional chopper between the 14V and 42V buses, duty ratio adjustment is utilized for power flow control between the two low-voltage buses, making the two bus voltages, V_{14V} and V_{42V} , track each other by

$$V_{14V} = d \cdot V_{42V}, \quad (1)$$

where d is the duty ratio of the switches S_1 and S_3 , defined as $d=t_{on}/T_{sw}$, where t_{on} is the conducting interval of S_1 and S_3 and T_{sw} the switching period as shown in Fig. 3. For 14V/42V systems, the duty ratio is fixed at $d=1/3$ for normal operation and can be changed to adjust the state of charge of the low-voltage batteries if necessary. It is noted that the two half-bridges operate at the same duty ratio.

In addition, a phase shift angle, ϕ , between the transformer primary and secondary voltages is employed for power flow control between the 42V and H.V. buses as shown in Fig. 3. For the discussion of the phase shift angle based power flow control, a simplified, primary-referred equivalent circuit is drawn in Fig. 4, where the half-bridges are simplified by a voltage source and L_s represents the leakage inductance of the transformer. At steady state, the voltages across the capacitors, C_1 and C_2 , C_3 and C_4 , and thus the positive and negative amplitudes of the voltage sources are determined by the duty ratio. For $d=1/3$, the voltage sources have positive and negative amplitudes of $2/3$ of and $1/3$ of the dc bus voltage, respectively. Idealized voltage and current waveforms of the transformer can then be illustrated in Fig. 5. Power flows from the 42V bus to the H.V. bus when the phase of the transformer primary voltage, v_{TrL} , supplied by the 42V half-bridge is leading the secondary voltage, v_{TrH} , supplied by the H.V. half-bridge. The converter thus works in the boost mode to power the H.V. bus. By making the phase of the secondary voltage, v_{TrH} , leading the primary voltage, v_{TrL} , power flow can be reversed.

The operation of the converter in one switching period can be divided into four intervals triggered by the switching instants and is represented by the four segments of the transformer current waveform in Fig. 5. A power flow equation can be derived from the relationships of the transformer voltages and current. Assuming the duty ratio is fixed at $1/3$, i.e., $\phi_{on}=2\pi/3$ at steady state, the power transferred through the transformer can be expressed by

$$P = \frac{V_{42V}V_{HV}}{n} \cdot \frac{\phi}{2\pi f_{sw} L_s} \cdot \left[\frac{2}{9} - \frac{\phi}{4\pi} \right], \quad (2)$$

where n is the transformer turns ratio, L_s is the transformer leakage inductance, and f_{sw} is the switching frequency.

For a given design, the maximum power is determined by

$$P_{max} = \frac{V_{42V}V_{HV}}{n} \cdot \frac{2}{81 f_{sw} L_s}, \quad (3)$$

$$\text{at } \phi_{P_{max}} = \frac{4\pi}{9}.$$

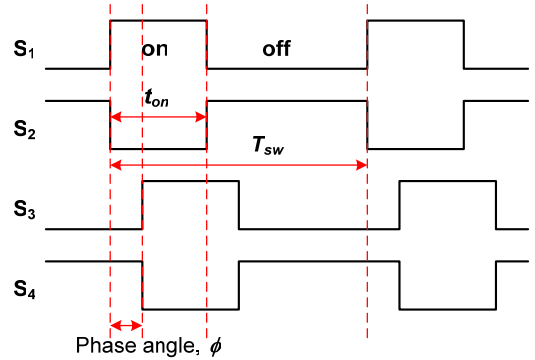


Fig. 3. Gating signals for power flow control based on adjusting the duty ratio and phase angle.

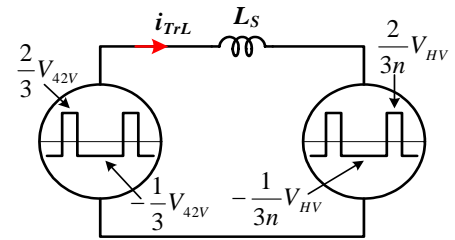


Fig. 4. Equivalent circuit for the 42V and H.V. buses at $d=1/3$.

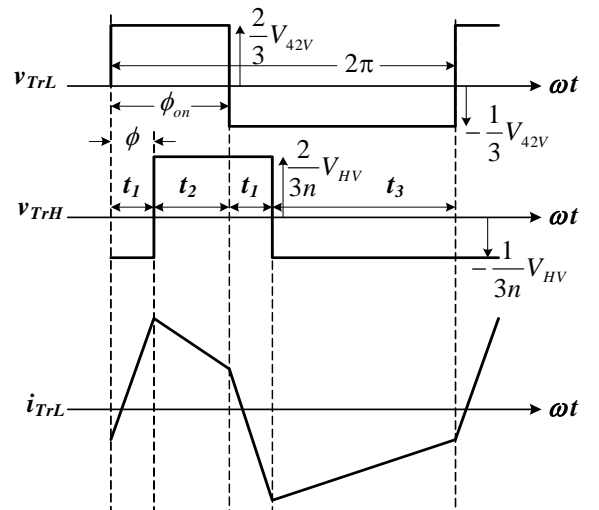


Fig. 5. Ideal transformer voltage and current waveforms illustrating power flow control between the 42V and H.V. buses at $d=1/3$.

Equation (2) indicates that, for a fixed duty cycle and switching frequency, the power is related to the phase shift angle and transformer leakage inductance. For a given amount of power, a smaller leakage inductance results in a smaller phase shift angle. To reduce the circulating current and to improve the efficiency, the phase shift angle should be kept as small as possible. Therefore, the leakage inductance needs to be minimized. On the other hand, a higher leakage inductance helps to meet the soft-switching conditions [5].

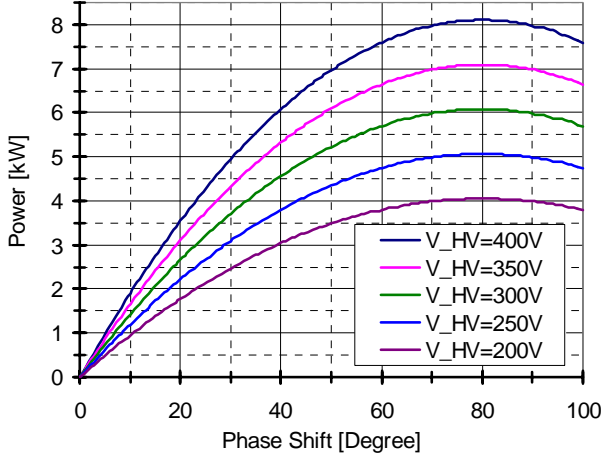


Fig. 6. Power transferred across the transformer vs. phase shift angle at various levels of V_{HV} , ($n=8$, $L_s=0.16\mu\text{H}$, $f_{sw}=40$ kHz, $V_{42V}=42\text{V}$).

Automotive applications usually require a peak power for a short period of time, typically in several tens seconds. Equation (3) can be used to help a design meet the peak

requirement. Fig. 6 plots the power transferred across the transformer versus the phase shift angle at different voltages of the H.V. bus, V_{HV} for a prototype design that specifies a continuous power of 2 kW and a peak value of 5 kW. With the design parameters: $n=8$, $L_s=0.16\mu\text{H}$, $f_{sw}=40$ kHz, $V_{42V}=42\text{V}$, it can meet the peak power requirement when the high voltage bus is over 250 V.

C. Configurations for HEVs and Fuel Cell Vehicles

Fig. 7 is a block diagram showing a configuration of the proposed dc/dc converter in HEV applications, where a 42 V alternator is the power source and the dc/dc converter provides power flow control for the 14 V and H.V. buses. The H.V. side switches, S_3 and S_4 can be replaced with diodes if power is not required to transfer from the H.V. bus to the 14V/42V buses. This configuration is particularly suitable for 42V integrated starter/alternator based mild hybrid utility and recreational vehicles that require an auxiliary ac power supply of 50Hz or 60Hz, i.e. a single phase inverter powered by the high voltage bus.

Fig. 8 illustrates the dc/dc converter in fuel cell powered vehicle applications, where a fuel cell stack is the power source, and the dc/dc converter provides power flow control for charging the 12 V and 36 V batteries during normal vehicle operations and for powering the H.V. bus for startup of the fuel cell stack.

III. SIMULATION AND EXPERIMENTAL RESULTS

Detailed circuit simulations were performed to verify the design goal of the prototype, which is to ensure that at

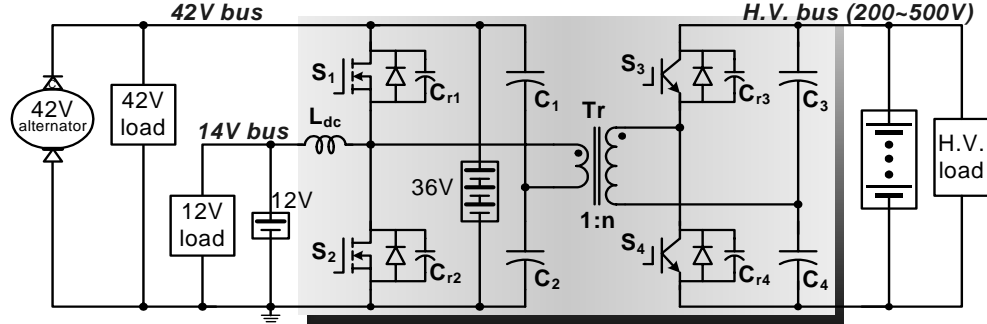


Fig. 7. The proposed dc/dc converter for HEV applications.

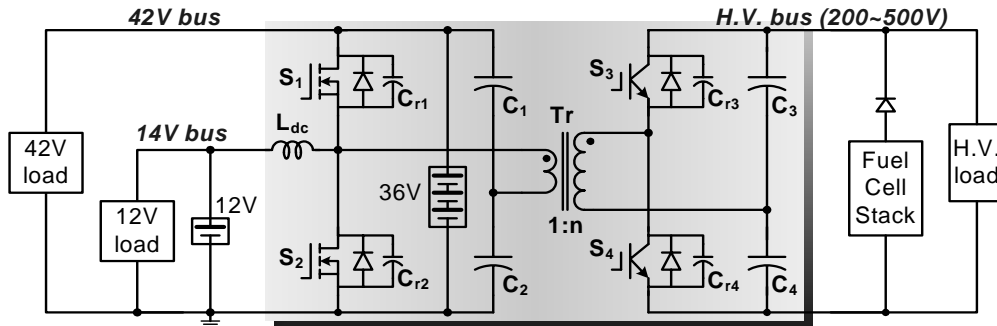
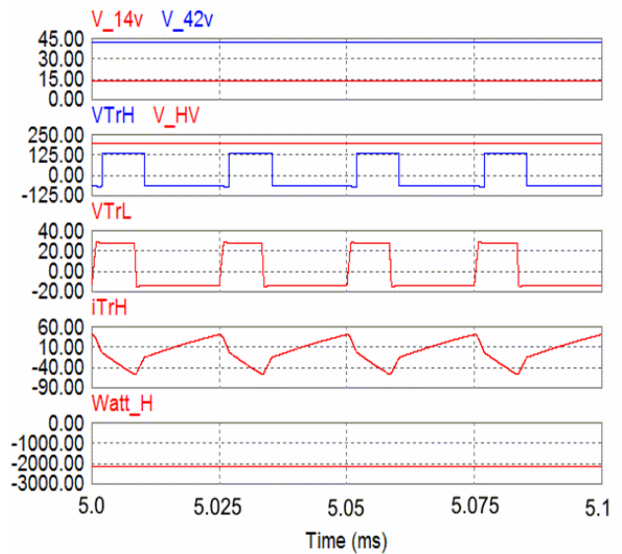


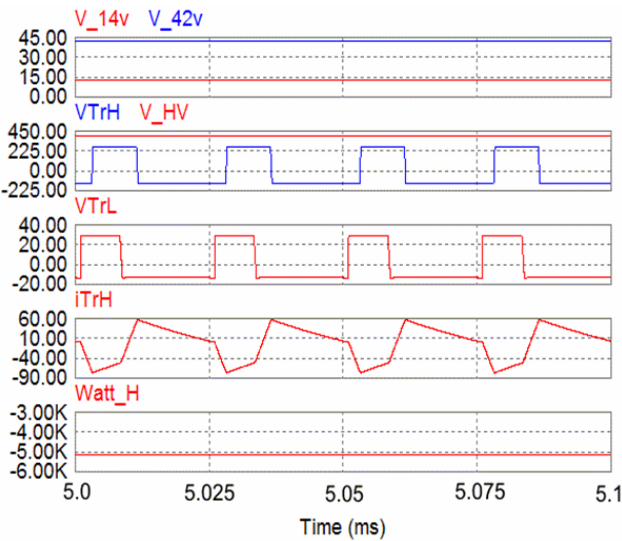
Fig. 8. The proposed dc/dc converter for fuel cell powered vehicle applications.

least 2 kW can be transferred in both directions at a voltage range of 200~400V for the H.V. bus. Figs. 9 and 10 are simulated waveforms, where V_{14v} , V_{42v} , V_{HV} , V_{TrH} , V_{TrL} , i_{TrH} , $Watt_H$, and $Watt_L$ represent the bus voltage of the 14V, 42V, H.V. buses, transformer primary and secondary voltages, secondary current, power transferred to the H.V., and 42V buses, respectively.

Fig. 9 shows the simulated results when power is transferred from the low voltage buses to the H.V. net. In (a), where the H.V. bus voltage, V_{HV} , is at the minimum value of 200V and the phase shift angle is set at 26.5 degrees, the amount of power transferred to the H.V. bus is 2.1 kW. In (b), V_{HV} is kept at 400V and 5.1 kW can be transferred to the H.V. bus at a phase angle of 34.6 degrees.

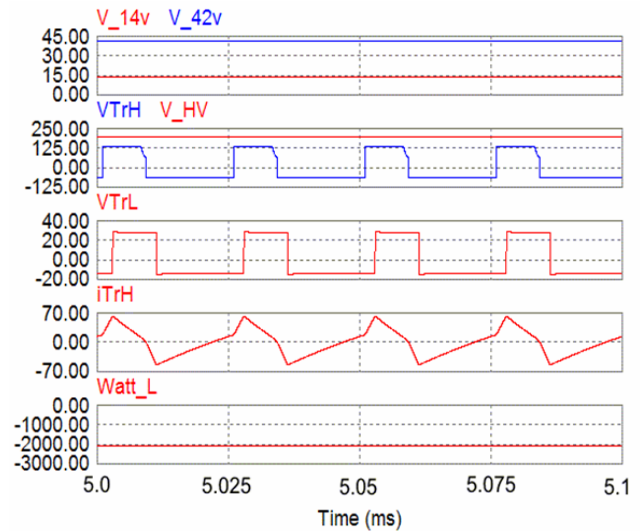


(a) $V_{HV}=200V$, power transferred to the H.V. bus: 2.1 kW.

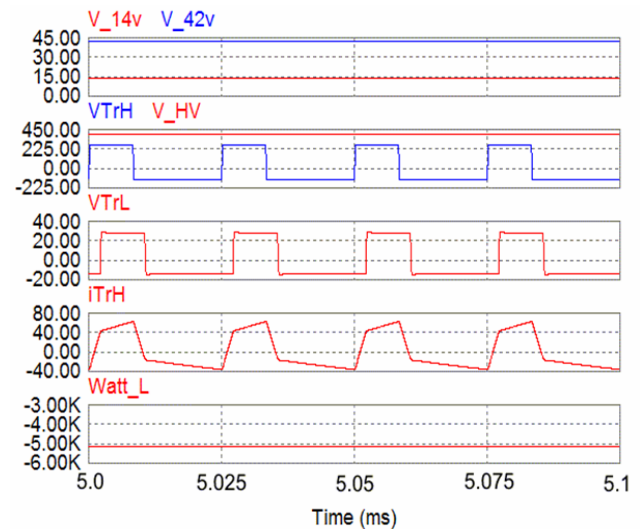


(b) $V_{HV}=400V$, power transferred to the H.V. bus: 5.1 kW.

Fig. 9. Simulation results showing power is transferred from the low voltage buses to the H.V. net.



(a) $V_{HV}=200V$, power transferred to the low voltage buses: 2.0 kW.



(b) $V_{HV}=400V$, power transferred to the low voltage buses: 5.1 kW.

Fig. 10. Simulation results illustrating power is transferred from the H.V. net to the low voltage buses.

The counterparts for reversed power flow are shown in Fig. 10. In (a), where V_{HV} is again at the minimum value of 200V, at the same phase shift angle of 26.5 degrees the amount of power transferred to the low voltage buses is 2.0 kW. In (b), where V_{HV} is kept at 400V and the phase angle is set at 34.9 degrees, 5.1 kW of power is transferred. The simulation results thus confirm the design goal.

A 2 kW lab unit was designed, built, and tested to verify the power flow control scheme. While the prototype design specifies a switching frequency of 40 kHz by using MOSFETs as both the low and H.V. switches, IGBTs were used for the high-voltage switches in the lab unit and the switching frequency was reduced to 22 kHz. Fig. 11 shows

a photo of the unit. All components are mounted on a water-cooled heat sink. The power flow control is implemented with a digital signal processor.

To verify the proposed power flow control scheme, the unit was tested by connecting a dc power supply at one bus and resistive loads at the other two buses. Fig. 12 shows experimental voltage and current waveforms when power flows from the 42V bus to the 14V and H.V. buses, where the amount of power transferred is 1.5 kW. The traces are, from top to bottom, the 14V, 42V, and H.V. buses voltage and current, V_{14V} and I_{14V} , V_{42V} and I_{42V} , V_{HV} and I_{HV} , the transformer secondary voltage and current, v_{TrH} and i_{TrH} , (for their polarity, refer to Fig. 2). Figs. 13 and 14 illustrate the same voltage and current waveforms for power flowing from the 14V bus to the 42V and H.V. buses, and from the H.V. bus to the 42V and 14V buses, respectively. The amount of power transferred is 1.2 kW and 850 W, respectively.

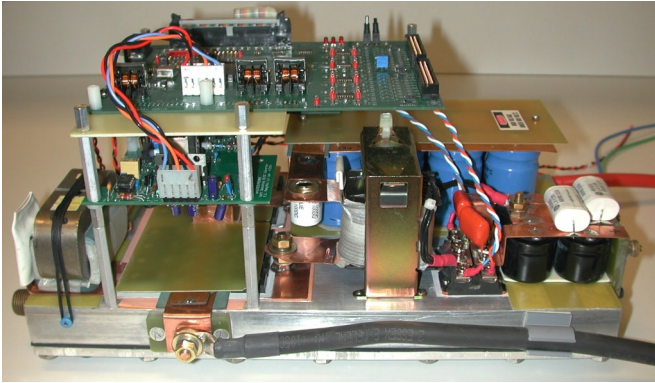


Fig. 11. Photo of the lab unit.

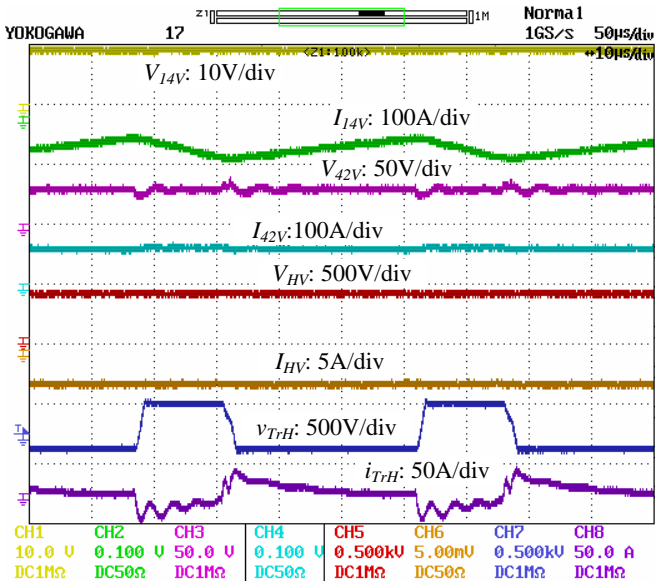


Fig. 12. Experimental waveforms for power flowing from the 42V bus to the 14V and H.V. buses. Time: 10μs/div.

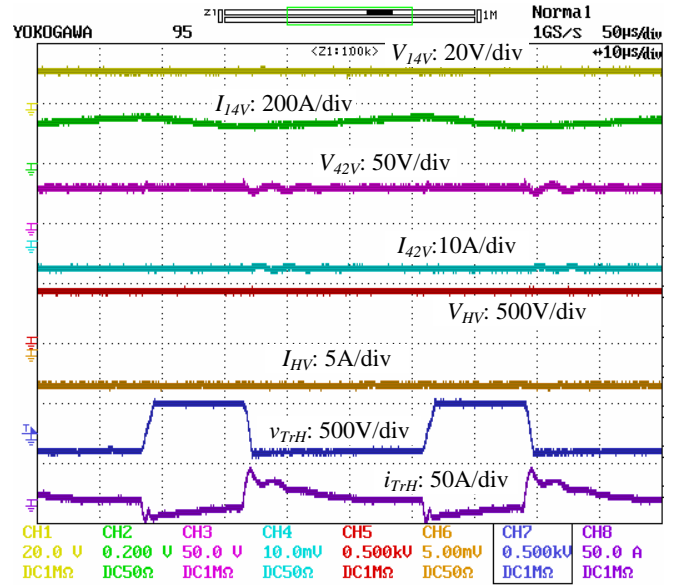


Fig. 13. Experimental waveforms for power flowing from the 14V bus to the 42V and H.V. buses. Time: 10μs/div.

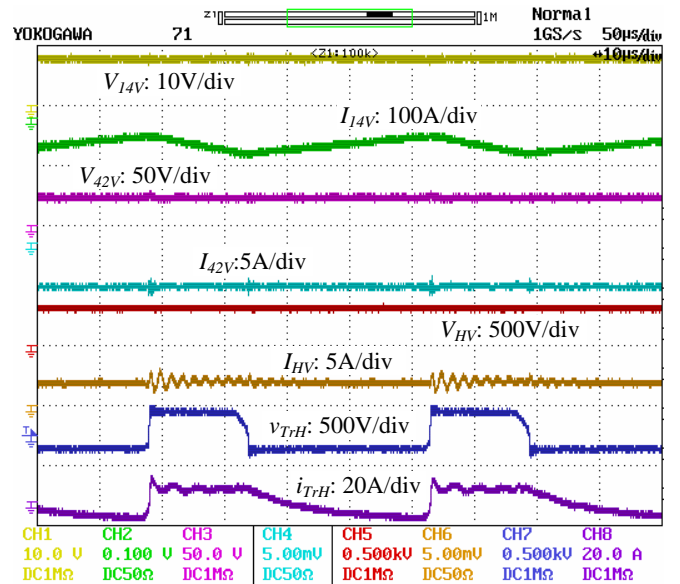


Fig. 14. Experimental waveforms for power flowing from the H.V. bus to the 42V and 14V buses. Time: 10μs/div.

IV. CONCLUSIONS

The proposed integrated dc/dc converter for triple-voltage-bus (14V/42V/H.V.) systems for automotive applications has the following features:

- Uses only four switching devices, leading to significant cost savings and higher power density.
- Requires no auxiliary circuits or complex control dedicated for soft switching.

- Flexible power flow management due to the capability of power transfer among all three voltage buses by employing the combined duty ratio and phase shift angle control scheme.

Simulation and experimental results on a 2 kW lab unit confirmed the operating principles of the converter.

REFERENCES

- [1] J. G. Kassakian, "Future Automotive Electrical Systems – The Power Electronics Market of the Future," Proceedings of the IEEE Applied Power Electronics Conference, New Orleans, Feb. 2000, pp. 3-9.
- [2] M. Naidu, R. Henry and N. Boules, "A 3.4 kW, 42 V, High efficiency automotive power generation system," SAE-FTT 2000 Conference, Aug. 20, 2000.
- [3] T. Gilchrist, "Fuel cells to the fore," *IEEE Spectrum*, November 1998.
- [4] M. H. K. Wang et al, "Bi-directional dc to dc converters for fuel cell systems," in *Conf. Rec. 1998 IEEE Power Electronics In Transportation*, pp. 47–51.
- [5] F. Z. Peng, H. Li, G. J. Su and J. S. Lawler, "A New ZVS Bi-directional dc-dc Converter for Fuel Cell and Battery Applications," *IEEE Trans. on Power Electronics*, vol. 19, no. 1, pp. 54-65, Jan. 2004.
- [6] D. M. Divan and O. Patterson, "A pseudo resonant full bridge dc/dc converter," in *Conf. Rec. 1987 IEEE Power Electronics Specialist Conf.*, pp. 424–430.
- [7] R. Watson et al., "A soft-switched, full-bridge boost converter employing an active-clamp circuit," in *Conf. Rec. 1996 IEEE Power Electronics Specialist Conf.*, pp. 1948–1954.
- [8] R. W. DeDonker, D. M. Divan, and Kheraluwala, "Power conversion apparatus for dc/dc conversion using dual active bridges," U. S. Patent, no. 5,027,264.